Direct Generation of Human Neuronal Cells from Adult Astrocytes by Small Molecules

Longfei Gao,[1] Wuqiang Guan,[2] Min Wang,[2] Huihan Wang,[3] Jiali Yu,[3] Qing Liu,[4] Binlong Qiu,[1] Yongchun Yu,[2] Yifang Ping,[4] Xiuwu Bian,[4] Li Shen,[3,*] and Gang Pei[1,5,*]

[1]State Key Laboratory of Cell Biology, CAS Center for Excellence in Molecular Cell Science, Institute of Biochemistry and Cell Biology, Chinese Academy of Sciences; University of Chinese Academy of Sciences, 320 Yueyang Road, Shanghai 200031, China
[2]Institute of Neurobiology, Institutes of Brain Science, State Key Laboratory of Medical Neurobiology and Collaborative Innovation Center for Brain Science, Fudan University, Shanghai 200032, China
[3]Life Sciences Institute, Zhejiang University, Hangzhou, Zhejiang 310058, China
[4]Institute of Pathology and Southwest Cancer Center, Southwest Hospital, Third Military Medical University, and Key Laboratory of Tumor Immunopathology, Ministry of Education of China, Chongqing 400038, China
[5]Shanghai Key Laboratory of Signaling and Disease Research, Collaborative Innovation Center for Brain Science, School of Life Sciences and Technology, Tongji University, Shanghai 200092, China
*Correspondence: li_shen@zju.edu.cn (L.S.), gpei@sibs.ac.cn (G.P.)
http://dx.doi.org/10.1016/j.stemcr.2017.01.014

SUMMARY

Astrocytes, due to the proximity to neuronal lineage and capability to proliferate, are ideal starting cells to regenerate neurons. Human fetal astrocytes have been successfully converted into neuronal cells by small molecules, which offered a broader range of further applications than transcription factor-mediated neuronal reprogramming. Here we report that human adult astrocytes could also be converted into neuronal cells by a different set of small molecules. These induced cells exhibited typical neuronal morphologies, expressed neuronal markers, and displayed neuronal electrophysiological properties. Genome-wide RNA-sequencing analysis showed that the global gene expression profile of induced neuronal cells resembled that of human embryonic stem cell-differentiated neurons. When transplanted into post-natal mouse brains, these induced neuronal cells could survive and become electrophysiologically mature. Altogether, our study provides a strategy to directly generate transgene-free neuronal cells from human adult astrocytes by small molecules.

INTRODUCTION

Neuron regeneration in adult mammalian brain is important for alleviation of brain injuries or neurodegenerative diseases. As the regeneration capacity of adult brains is limited (Goldman, 2016), cell replacement therapy using exogenous cells seems promising. Among them, neuronal cells differentiated from stem cells offer great hopes for restoring neuronal function (Lindvall and Kokaia, 2006), and transcription factor (TF)-mediated neuronal reprogramming from terminal differentiated somatic cells also provides an alternative strategy to generate functional neurons (Goldman, 2016; Mertens et al., 2016; Yang et al., 2011). However, potential risks such as tumorigenesis and the difficulty of delivering them into the brain are obstacles preventing their applications. Alternatively, small molecules, the biological effects of which are generally reversible and finely tunable, could reprogram fibroblasts into neural progenitor or neuronal cells without integration of ectopic transgenes (Cheng et al., 2014; Hu et al., 2015; Li et al., 2015; Zhang et al., 2016a), opening a new avenue for neuron regeneration.

Astrocytes, the most abundant cell types in the brain, play important roles in maintaining brain homeostasis and modulating neural circuit activity (Clarke and Barres, 2013). Astrocytes developmentally originate from the same precursor cells as neurons, are capable of proliferating

in response to brain damages, and therefore are considered as ideal starting cells to regenerate neurons (Amamoto and Arlotta, 2014; Chouchane and Costa, 2012). Previous reports found that mouse astrocytes could be converted into neuronal cells in vitro and in vivo by forced expression of TFs (Berninger et al., 2007; Guo et al., 2014; Heinrich et al., 2010, 2011; Liu et al., 2015; Niu et al., 2013). Moreover, genetically unmodified neuronal cells could be derived from mouse astrocytes and human fetal astrocytes with small molecules (Cheng et al., 2015; Zhang et al., 2015), demonstrating the feasibility of small-molecule-mediated astrocytic-neuronal conversion. However, in addition to the potential ethical concerns of using embryos and the immune rejection of allotransplantation, fetal astrocytes may exhibit properties distinct from adult astrocytes (Zhang et al., 2016b). Here, we demonstrate that human adult astrocytes could be directly converted into transgene-free neuronal cells by a set of small molecules.

RESULTS

Characterization of Cultured Human Adult Astrocytes

Human adult astrocytes were derived from neuropathologist-confirmed normal brain tissues. To avoid the presence of neural progenitor cells (NPCs) in the cultured cells, only brain regions where NPCs are not enriched were used, and
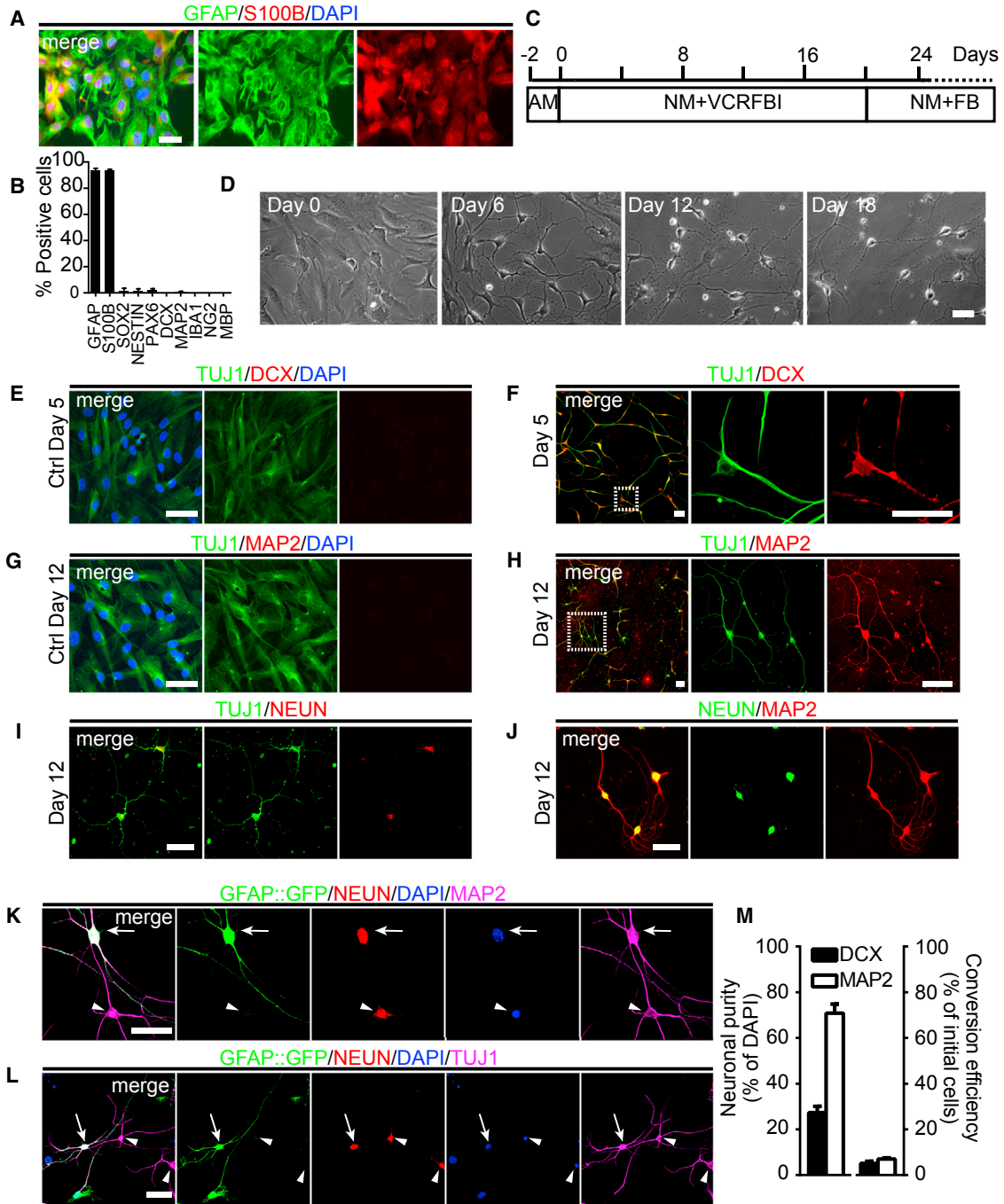
CrossMark

Figure 1. Conversion of Human Adult Astrocytes into Neuronal Cells by Small Molecules under Defined Conditions

(A) Immunostaining showing the cultured cells expressed astrocyte markers GFAP and S100B.

(B) The cultured cells expressed astrocyte markers, but not markers for NPCs, neuronal cells, or other glial cells. Average percentages of cells expressing the indicated neural markers are shown (mean ± SEM, n = 3 independent experiments).

(C) Schematic diagram showing the neuronal induction protocol. AM, astrocyte growth medium; NM, neuronal medium; V, VPA; C, Chir99021; R, Repsox; F, forskolin; B, i-Bet151; I, ISX-9.

(D) Cells changed from astrocytic morphology to neuronal morphology along the induction process. Representative images at day 0, 6, 12, and 18 are shown.

(E and F) Immunostaining of control cells (E) and small-molecule-treated cells (F) at day 5 with TUJ1 and DCX antibodies.

(legend continued on next page)

the cells were maintained and expanded in a medium containing fetal bovine serum, which stimulates differentiation of NPCs. Indeed, the cultured cells were unable to form neurospheres and neuronal cells were not detectable after culturing the cells in the neuronal differentiation medium for 1 month (Figures S1I–S1K). Thus, NPCs did not seem to be present in the cultured cells. About 95% of the cells expressed astrocytic markers GFAP and S100B (Figures 1A and 1B), and more than 80% were positive for CD44 (Figures S1F and S1G), which is expressed by human astrocytes but not by NPCs or neuronal cells (Moretto et al., 1993; Yuan et al., 2011). In addition, the cultured cells were negative for the neuronal markers DCX or MAP2, microglial marker IBA1, NG2 glial marker NG2, or oligodendrocyte marker MBP (Figures 1B and S1B–S1E). These results collectively suggested that the cultured cells were astrocytes without detectable contamination of NPCs, neuronal cells, or other glial cells.

Consistent with previous reports that astrocytes could express pro-inflammatory genes in response to IL1β stimulation (Caiazzo et al., 2015), pro-inflammatory genes including *IL1B*, *IL6*, and *COX2* were significantly upregulated upon IL1β stimulation (Figure S1H), demonstrating that the cultured cells are indeed functional astrocytes.

Small-Molecule-Treated Human Adult Astrocytes Acquired Neuronal Properties

As the VCR cocktail (Valproic acid, Chir99021, and Repsox), which induced mouse astrocytes into neuronal cells (Cheng et al., 2015), was not able to induce obvious morphological change on cultured human astrocytes (data not shown), we treated cultured astrocytes with more small molecules that are frequently used in neuronal reprogramming or differentiation together with VCR. The combination containing three additional small molecules (forskolin, i-Bet151, and ISX-9) could dramatically change the cell morphology into bipolar or multipolar shapes after treatment for 2 days (data not shown). Upon prolonged treatment, cell bodies became smaller and more compact, showing complicated neurite-like structures (Figure 1D). In contrast, no significant morphological change was observed in the control group where small molecules were not added (Figures 1E and 1G). Immunostaining results revealed that DCX was detectable at day 5 post

small-molecule induction (Figure 1F), and MAP2 and NEUN were detectable at day 12 (Figures 1H–1J). However, neither DCX nor MAP2 was detectable in the control group (Figures 1E and 1G). These data indicated that adult astrocytes acquired a neuronal fate after small-molecule treatment. Based on MAP2 expression and cell morphology, the neuronal purity and conversion efficiency were estimated to be about 70% and 8%, respectively (Figure 1M). Similar results were also obtained when using adult astrocytes from another donor as starting cells (Figures S2A–S2C), demonstrating that astrocytes from different individuals could also be chemically induced into neuronal cells. However, removing any of the small molecules impaired the conversion efficiency and neuronal purity (Figure S2K), indicating that all small molecules were important for the conversion. Interestingly, TUJ1, another neuronal marker, was positive in both small-molecule-treated and untreated groups (Figures 1E–1H), indicating that the induction medium itself could activate *TUJ1* expression. Thus, multiple makers as well as morphological features should be examined when defining induced neurons (Yang et al., 2011).

We further traced the cultured astrocytes with retrovirus expressing GFP from human GFAP promoter (GFAP:GFP) as described previously (Cheng et al., 2015; Guo et al., 2014; Zhang et al., 2015). When GFAP::GFP-traced astrocytes were used as starting cells, GFP was readily detectable in some MAP2- and NEUN-positive cells 12 days after induction (Figures 1K and 1L), similar to previously reported astrocytic-neuronal conversions (Guo et al., 2014; Zhang et al., 2015). These findings confirmed that the neuronal cells were converted from GFAP-positive astrocytes.

Neuronal Cells Derived from Human Adult Astrocytes Showed Functional Maturation

At day 30 the induced neuronal cells exhibited typical neuronal morphology and were positive for MAP2, NEUN, SYN1, and TAU (Figures 2A–2E). The induced neuronal cells generated repetitive trains of action potentials (APs) elicited by injected step currents (86.2%, n = 29) (Figures 2F and 2G). The average resting membrane potential (RMP), AP threshold, and AP amplitude were about −64.4 ± 1.71, −42.5 ± 1.20, and 36.5 ± 2.23 mV, respectively (mean ± SEM; n = 39, 25, and 25) (Figure 2J).

(G–J) Immunostaining of control cells (G) and small-molecule-treated cells (H), (I), and (J) at day 12 with TUJ1, MAP2, and NEUN antibodies.

(K and L) Induced neuronal cells were originated from GFAP-positive astrocytes. The starting astrocytes were traced with GFAP::GFP retrovirus. After induction for 12 days, GFP remained detectable in some NEUN-positive cells (arrows), although it was silenced in other NEUN-positive cells (triangles).

(M) Quantification of neuronal purity and conversion efficiency (mean ± SEM, n = 3 independent experiments).

Representative images of n = 3 independent experiments are shown in (A), (D), (K), and (L) and of n = 4 independent experiments in (E), (F), (G), (H), (I), and (J). Scale bars, 50 μm. See also Figures S1–S3.
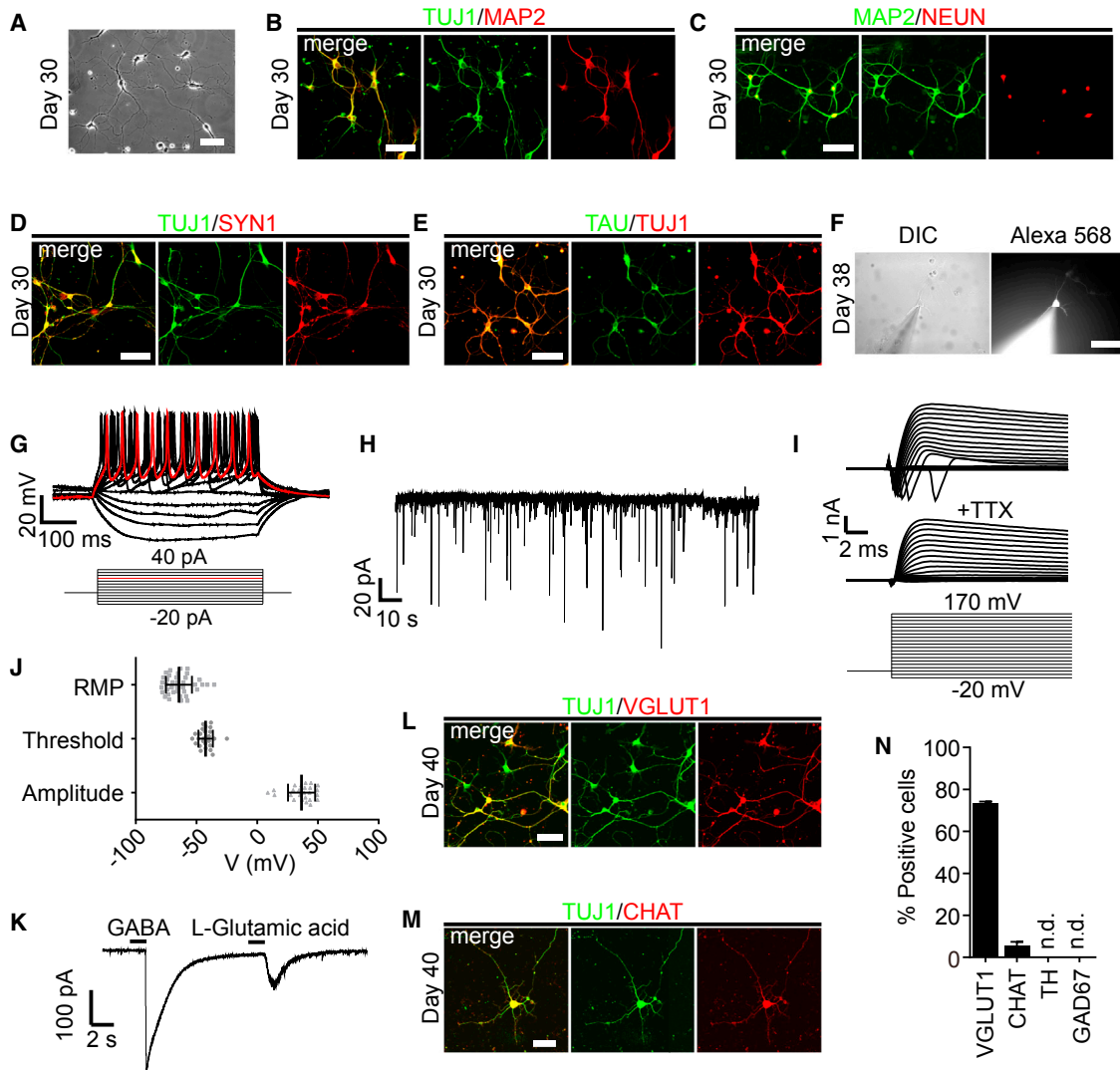
Figure 2. Functional Maturation of Adult Astrocyte-Induced Human Neuronal Cells

(A–E) Induced cells displayed typical neuronal morphology and expressed mature neuronal markers at day 30. Representative images of n = 3 independent experiments are shown. Scale bars, 50 μm.

(F) Patch clamp recordings were conducted on induced neuronal cells at day 38. Scale bar, 50 μm.

(G) Representative traces of APs recorded on induced neuronal cells when injected with step currents. An exemplary trace was highlighted in red (n = 29).

(H) Representative traces of sPSCs on induced neuronal cells (n = 23).

(I) Representative inward sodium currents elicited by injected step voltage on induced neuronal cells (n = 21). The inward currents could be blocked by Na$^+$ channel blocker tetrodotoxin (TTX).

(J) Quantification of RMP (n = 39), AP threshold (n = 25), and AP amplitude (n = 25) of induced neuronal cells (mean ± SEM).

(K) Focal application of L-glutamic acid (n = 11) or GABA (n = 8) induced inward membrane currents.

(L–N) The induced neuronal cells were mainly glutamatergic neurons. Immunostaining against specific neuronal subtype markers was performed at day 40 (L) and (M), and quantification (N) was performed (mean ± SEM, n = 3 independent experiments). n.d., not detectable. Scale bar, 50 μm.

See also Figure S2.

Inward sodium currents were also elicited by injected step voltage (85.7% positive, n = 21), and could be blocked by Na$^+$ channel blocker tetrodotoxin (Figure 2I). In addition, these neuronal cells showed typical spontaneous post-synaptic currents (sPSCs) (82.6%, n = 23) (Figure 2H), and inward membrane currents could also be induced when
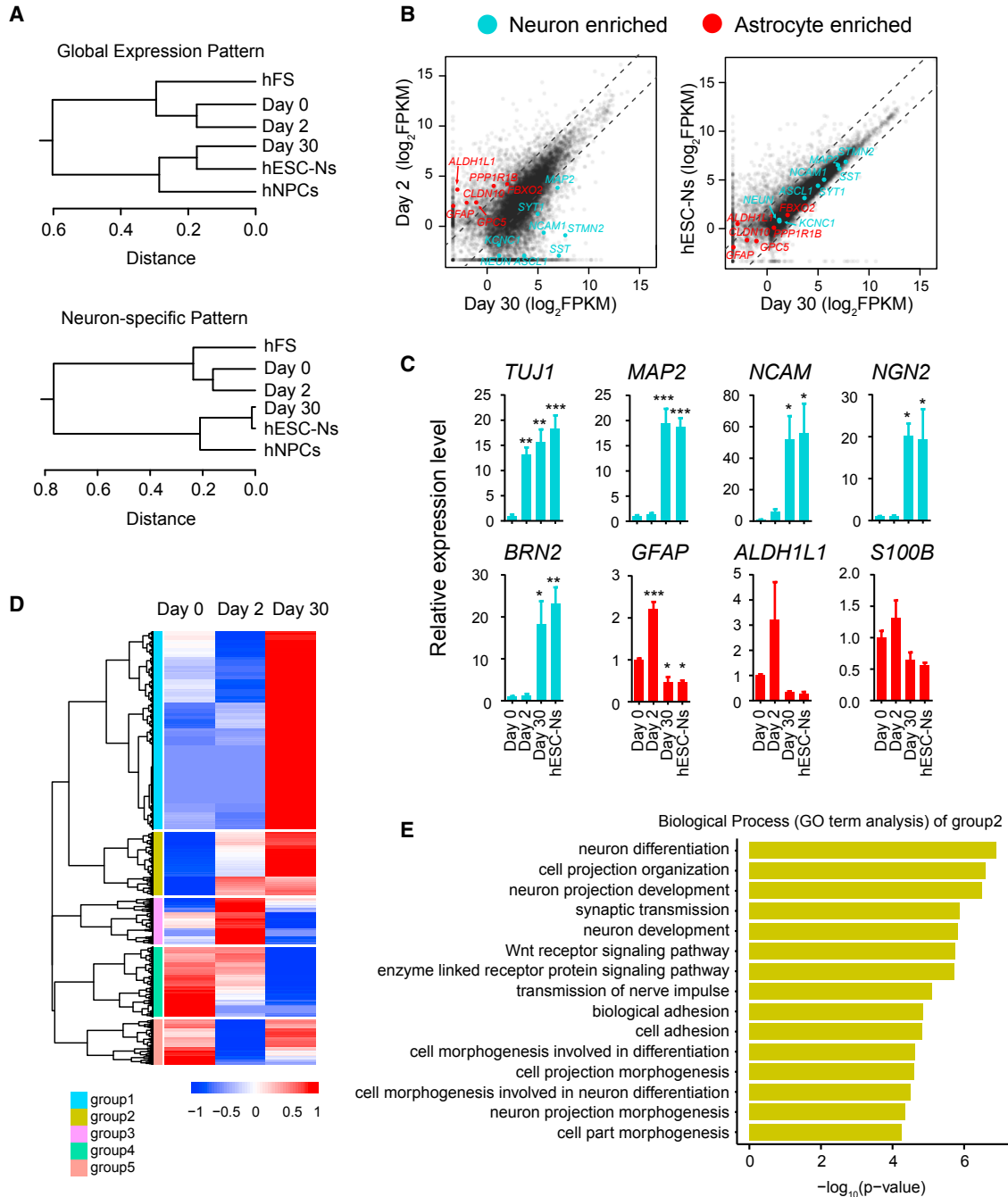
Figure 3. Transcriptome Analysis of Induced Neuronal Cells

(A) Hierarchical clustering of starting astrocytes (day 0), astrocytes treated with small molecules for 2 days (day 2), astrocyte-derived neuronal cells (day 30), hESC-differentiated NPCs (hNPCs), and CD24+ neurons (hESC-Ns), as well as human adult fibroblasts (hFS).

(B) Scatterplots comparing gene expression levels between day 30 neuronal cells and day 2 astrocytes (left panel) or hESC-Ns (right panel). Astrocyte-enriched genes are highlighted in red and neuron-enriched genes in cyan. Dashed line indicates a 4-fold change.

(C) Real-time PCR validation of the expression of representative astrocyte- and neuron-enriched genes. Astrocyte-enriched genes were shown in red and neuron-enriched genes in cyan. Data were shown as fold change versus day 0 (mean ± SEM, n = 3 independent experiments, *p < 0.05; **p < 0.01; ***p < 0.001; versus day 0 sample).

(legend continued on next page)

exogenous L-glutamic acid (90.9%, n = 11) or GABA (100%, n = 8) were puffed onto induced neuronal cells (Figure 2K). These data collectively indicated that the induced neuronal cells were capable of exhibiting electrophysiological activities and forming synaptic connections.

Interestingly, up to 70% of the neuronal cells were VGULT1 positive and about 7% were CHAT positive at day 40 (Figures 2L–2N), while dopaminergic neuron marker TH or GABAergic neuron marker GAD67 was not detectable (Figures 2N, S2D, and S2E), suggesting that human adult astrocytes were mainly reprogrammed into glutamatergic neurons here.

Generation of Neuronal Cells from Human Adult Astrocytes Might Not Pass through the NPC Stage

Although neuronal TFs such as *NEUROD1*, *NGN2*, and *ASCL1* were significantly upregulated from day 0 to day 5, NPC markers *SOX2* and *NESTIN* remained at low expression levels and were not detectable by immunostaining (Figures S3A–S3D). Exploration of gene expression dynamics along the entire conversion process revealed that neuronal genes (e.g., *NGN2*, *ASCL1*, *MAP2*, and *SYN1*) were significantly upregulated (Figure S3E), and astrocyte genes (e.g., *GFAP*, *S100B*, and *ALDH1L1*) were downregulated (Figure S3F), while the expression levels of NPC markers (e.g., *NESTIN*, *SOX2*, *SOX1*, and *PAX6*) were not altered and were much lower than those in human NPCs (Figure S3G). Consistently, cell proliferation was not observed during the conversion process (Figures S3H and S3I), although cell death could be detected at the early induction stage (Figures S3J and S3K). Collectively, our results suggested that the conversion process might not pass through the NPC stage.

Genome-wide Transcriptome Profile of Induced Neuronal Cells Resembled that of Human Embryonic Stem Cell-Differentiated Neurons

We then generated human embryonic stem cell (hESC)-differentiated NPCs (hNPCs) and CD24+ neurons (hESC-Ns) as reported previously (Hu et al., 2015; Pruszak et al., 2007; Zhang et al., 2013) (Figures S4A–S4G), and performed RNA-sequencing (RNA-seq) analyses together with astrocyte-derived neuronal cells (day 30), starting astrocytes (day 0), astrocytes treated with small molecules for 2 days (day 2), as well as human adult fibroblasts (hFS). Unsupervised clustering showed that day 30 neuronal cells shared a similar gene expression pattern to that of hESC-Ns,

and were grouped together with hESC-Ns but apart from day 0 or day 2 astrocytes (Figures 3A and S4H). Although day 2 astrocytes had started to exhibit bipolar or multipolar morphology, their transcriptome was still similar to that of day 0 astrocytes (Figures 3A and S4H). Interestingly, day 0 and day 2 astrocytes were more distant from hNPCs than from hFS, while day 30 neuronal cells were more distant from hFS than from hNPCs, demonstrating that the transcriptome profile dramatically changed during the conversion process (Figure 3A).

After prolonged small-molecule treatment, the expression levels of astrocyte-enriched genes such as *GFAP* and *ALDH1L1* were decreased; however, neuron-enriched genes including *MAP2*, *NEUN*, and others were significantly upregulated (Figure 3B, left panel). Neuron-enriched genes were expressed at a higher level than astrocyte-enriched genes in both day 30 neuronal cells and hESC-Ns, without significant difference between these two types of cells (Figure 3B, right panel). After RT-qPCR validation of the RNA-seq results (Figure 3C), we performed pairwise comparison among the transcriptomes of day 0 and day 2 astrocytes and day 30 neuronal cells, and identified 6,701 differentially expressed genes (DEGs) (fold change >4, fragments per kilobase of transcript per million mapped reads [FPKM] >1) that could be classified into five groups by unsupervised hierarchical cluster analysis (Figure 3D). Of these 6,701 DEGs, 997 were activated at day 2, and remained highly expressed in day 30 neuronal cells (group 2). Gene ontology analysis revealed that these genes were significantly enriched in neuron development/differentiation, neuron morphology, and synaptic transmission processes (Figure 3E), suggesting that neuronal conversion started as early as day 2. These results demonstrated that the transcription regulatory network of human adult astrocytes was fully reprogrammed toward that of neuronal lineage under our induction conditions.

Survival and Electrophysiological Maturation of Induced Neuronal Cells in Mouse Brains

Adult astrocytes were labeled with GFP by lentivirus and induced by small molecules for 6 days (Figures S2F–S2H), and then trypsinized and injected into the lateral ventricle of post-natal day 1 mice (Figure 4A). At day 7 post injection (7 DPI), the transplanted cells could be observed and were positively stained for human nuclei (Figure 4B). DCX and NEUN were also positive in some of the surviving cells (Figures 4C and 4D). At 15, 30, and 42 DPI, some

(D) Heatmap illustration showing DEGs (fold change >4, FPKM >1 in at least one sample) obtained by a pairwise comparison among day 0, day 2, and day 30 cells. A total of 6,701 DEGs were classified into five groups by unsupervised hierarchical clustering.
(E) Gene ontology analysis of the group 2 genes classified in (D).
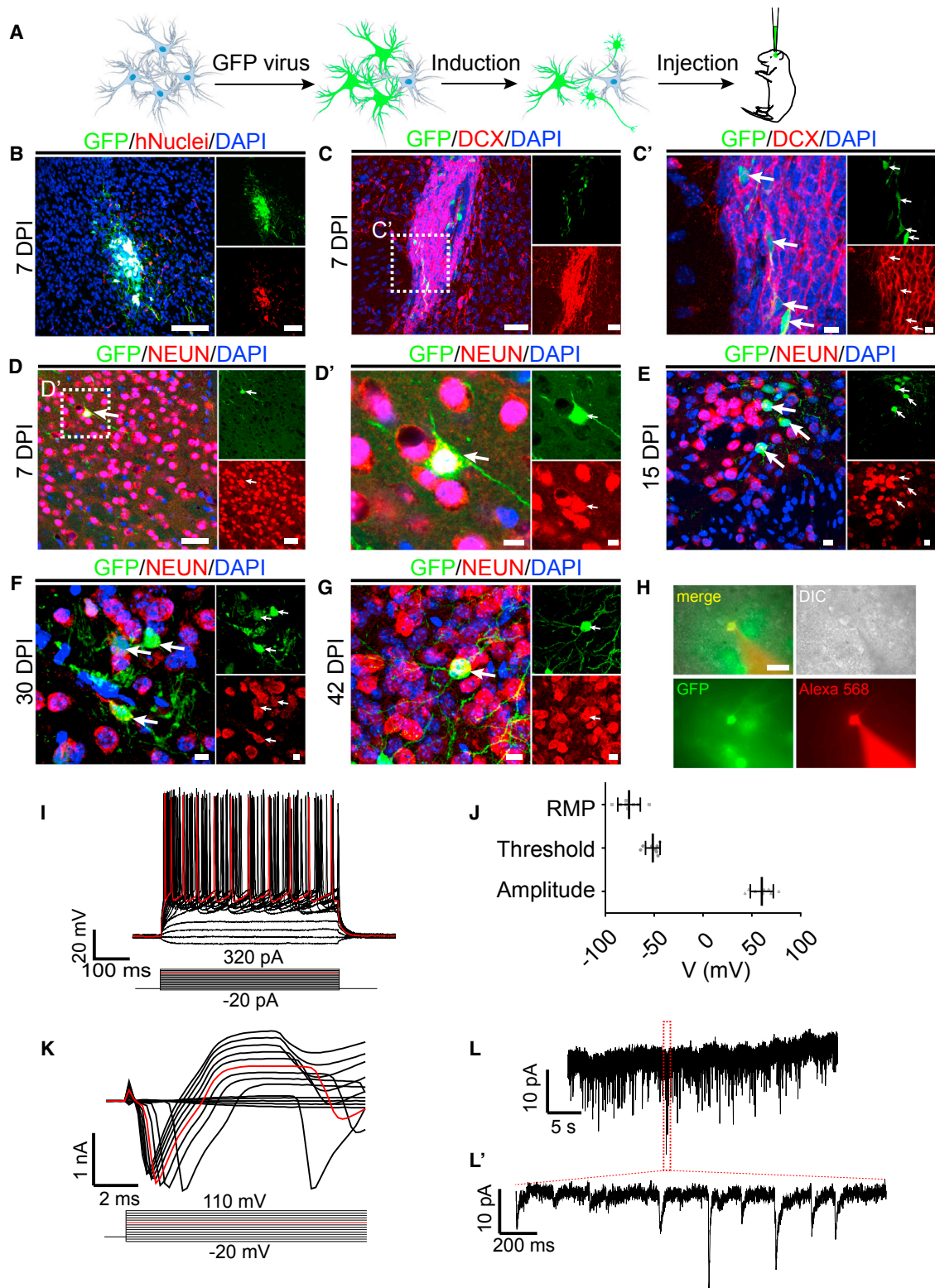See also Figure S4.

Figure 4. Survival and Electrophysiological Maturation of Induced Neuronal Cells in Mouse Brains

(A) Schematic diagram showing the experimental procedure of intracerebral injection of induced cells.

(B and C) Immunostaining against human nuclei (hNuclei) and DCX (C), (C′) in mouse brain at 7 days post injection (DPI).

(legend continued on next page)

transplanted cells were positive for NEUN and displayed typical neuronal morphology with complex neurites (Figures 4E–4G). At 48 DPI, electrophysiological recordings revealed that they fired repetitive trains of APs when injected with step currents (Figures 4H and 4I, n = 8). The RMP, AP threshold, and AP amplitude were about −75.7 ± 4.10, −51.4 ± 2.62, and 60.3 ± 4.15 mV (mean ± SEM, n = 8, 8, and 8), respectively (Figure 4J). Inward sodium currents were also elicited by injected step voltage (Figure 4K, n = 4). These cells also exhibited typical sPSCs (Figures 4L and 4L′, n = 4). These results suggested that induced neuronal cells could survive and became electrophysiologically mature in mouse brains.

DISCUSSION

Human fetal astrocytes could be reprogrammed into neuronal cells by the chemical cocktail MCM (Zhang et al., 2015). Here we further converted human adult astrocytes into neuronal cells with a different set of small molecules, providing a more fascinating prospect by avoiding potential immune rejection and ethical issues. Human adult astrocytes showed little morphological change after MCM treatment, while human fetal astrocytes died dramatically when treated with our chemical cocktail (data not shown), suggesting that human fetal and adult astrocytes bear unique traits (Zhang et al., 2016b). Unlike fetal astrocytes, human adult astrocytes could not spontaneously transform into DCX- or MAP2-positive cells without small-molecule treatment. These results were in accordance with the general belief that adult cells are more resistant to being reprogrammed compared with their fetal counterparts (Chung et al., 2014).

TFs are considered as the major determinants of specific cell lineages and lineage conversions (Mertens et al., 2016; Xu et al., 2015), and small molecules enabled TFs to induce neuronal conversion more efficiently (Gascón et al., 2016; Ladewig et al., 2012; Liu et al., 2013). However, this study together with previous reports further showed that, without ectopic expression of TFs, specific small molecules could activate key neuronal TFs in fibroblasts or astrocytes to reprogram them into neuronal cells (Cheng et al., 2015; Hu et al., 2015; Li et al., 2015; Zhang et al.,

2015). Among the chemicals used in this study, ISX-9 activated neuronal genes while i-Bet151 suppressed astrocyte genes (Figure S2J), consistent with previous report that ISX-9 activated the neuronal network and i-BET151 disrupted the original fibroblast core transcriptional network (Li et al., 2015); VPA, which was reported to promote neurogenesis and neuronal maturation (Hsieh et al., 2004; Niu et al., 2013), functioned to activate neuronal genes (Figure S2J); and forskolin, which was reported to reduce lipid peroxidation and promote neuronal conversion efficiency (Gascón et al., 2016; Liu et al., 2013), was important for cell morphology changes (Figure S2I). Importantly, removing Chir99021 and Repsox, the glycogen synthase kinase 3β, and transforming growth factor β inhibitors, which were thought to enhance TF-driven neuronal conversion efficiency (Ladewig et al., 2012), resulted in complete failure of our chemical-mediated neuronal conversion (data not shown), suggesting their essential roles. Therefore, the comprehensive roles and synergetic effects of these small molecules in chemical-mediated neuronal conversion remain to be further investigated.

Our RNA-seq data showed that the induced neuronal cells shared a highly similar gene expression pattern to hESC-differentiated neurons, together with our other results, demonstrating small-molecule-mediated astrocytic-neuronal conversion was a feasible way to generate neuronal cells. However, some signaling pathways or epigenetic modifications may need to be elaborately modulated by finely tuning the small molecules to generate specific subtypes of neurons. Moreover, whether the small molecules used here could reprogram resident astrocytes into neuronal cells in vivo and therefore help against neurological diseases or brain injuries remains to be answered.

EXPERIMENTAL PROCEDURES

Induction of Neuronal Cells from Human Adult Astrocytes

Human adult astrocytes were obtained with written consent from the patients or their guardians as approved by the ethics committees of the Third Military Medical University. The cells were maintained and expanded in human astrocyte growth medium. For

---

(D–G) Immunostaining against NEUN at 7 (D), (D′), 15 (E), 30 (F), and 42 (G) DPI.

The arrows indicate transplanted cells that were positive for DCX (C′) or NEUN (D, D′, E, F, G). Scale bars, 50 μm (B), (C), (D) or 10 μm (C′), (D′), (E), (F), (G). Representative images of n = 3 independent experiments are shown.

(H) Electrophysiological properties of transplanted cells were analyzed on acute slices at 48 DPI. Scale bar, 50 μm.

(I) Representative trace of APs recorded on transplanted cells when injected with step currents (n = 8).

(J) Quantification of average RMP, AP threshold, and AP amplitude of transplanted cells (mean ± SEM, n = 8, 8, and 8).

(K) Representative inward sodium currents elicited by injected step voltage on transplanted cells (n = 4).

(L, L′) Representative trace of sPSCs on transplanted cell (n = 4).

See also Figure S2.

neuronal conversion, astrocytes were seeded on poly-D-lysine-treated coverslips in growth medium. Two days later, induction medium containing small molecules was added. The induction medium was changed every 4 days. Detailed induction procedures are provided in Supplemental Experimental Procedures.

Statistical Analysis

All quantified data were statistically analyzed and presented as mean ± SEM. Two-tailed Student's t tests were used to calculate statistical significance with p values. A p value < 0.05 was considered statistically significant.

ACCESSION NUMBERS

The accession number for the RNA-seq dataset in this study is GEO: GSE84826.

SUPPLEMENTAL INFORMATION

Supplemental Information includes Supplemental Experimental Procedures, four figures, and one table and can be found with this article online at http://dx.doi.org/10.1016/j.stemcr.2017.01.014.

AUTHOR CONTRIBUTIONS

ACKNOWLEDGMENTS

REFERENCES

Amamoto, R., and Arlotta, P. (2014). Development-Inspired reprogramming of the mammalian central nervous system. Science 343, 1239882.

Berninger, B., Costa, M.R., Koch, U., Schroeder, T., Sutor, B., Grothe, B., and Gotz, M. (2007). Functional properties of neurons derived from in vitro reprogrammed postnatal astroglia. J. Neurosci. 27, 8654–8664.

Caiazzo, M., Giannelli, S., Valente, P., Lignani, G., Carissimo, A., Sessa, A., Colasante, G., Bartolomeo, R., Massimino, L., Ferroni, S., et al. (2015). Direct conversion of fibroblasts into functional astrocytes by defined transcription factors. Stem Cell Rep. 4, 25–36.

Cheng, L., Hu, W., Qiu, B., Zhao, J., Yu, Y., Guan, W., Wang, M., Yang, W., and Pei, G. (2014). Generation of neural progenitor cells by chemical cocktails and hypoxia. Cell Res. 24, 665–679.

Cheng, L., Gao, L., Guan, W., Mao, J., Hu, W., Qiu, B., Zhao, J., Yu, Y., and Pei, G. (2015). Direct conversion of astrocytes into neuronal cells by drug cocktail. Cell Res. 25, 1269–1272.

Chouchane, M., and Costa, M.R. (2012). Cell therapy for stroke: use of local astrocytes. Front. Cell. Neurosci. 6, 49.

Chung, Y.G., Eum, J.H., Lee, J.E., Shim, S.H., Sepilian, V., Hong, S.W., Lee, Y., Treff, N.R., Choi, Y.H., Kimbrel, E.A., et al. (2014). Human somatic cell nuclear transfer using adult cells. Cell Stem Cell 14, 777–780.

Clarke, L.E., and Barres, B.A. (2013). Emerging roles of astrocytes in neural circuit development. Nat. Rev. Neurosci. 14, 311–321.

Gascón, S., Murenu, E., Masserdotti, G., Ortega, F., Russo, G.L., Petrik, D., Deshpande, A., Heinrich, C., Karow, M., Robertson, S.P., et al. (2016). Identification and successful negotiation of a metabolic checkpoint in direct neuronal reprogramming. Cell Stem Cell 18, 396–409.

Goldman, S.A. (2016). Stem and progenitor cell-based therapy of the central nervous system: hopes, hype, and wishful thinking. Cell Stem Cell 18, 174–188.

Guo, Z., Zhang, L., Wu, Z., Chen, Y., Wang, F., and Chen, G. (2014). In vivo direct reprogramming of reactive glial cells into functional neurons after brain injury and in an Alzheimer's disease model. Cell Stem Cell 14, 188–202.

Heinrich, C., Blum, R., Gascón, S., Masserdotti, G., Tripathi, P., Sánchez, R., Tiedt, S., Schroeder, T., Götz, M., and Berninger, B. (2010). Directing astroglia from the cerebral cortex into subtype specific functional neurons. PLoS Biol. 8, e1000373.

Heinrich, C., Gascón, S., Masserdotti, G., Lepier, A., Sanchez, R., Simon-Ebert, T., Schroeder, T., Götz, M., and Berninger, B. (2011). Generation of subtype-specific neurons from postnatal astroglia of the mouse cerebral cortex. Nat. Protoc. 6, 214–228.

Hsieh, J., Nakashima, K., Kuwabara, T., Mejia, E., and Gage, F.H. (2004). Histone deacetylase inhibition-mediated neuronal differentiation of multipotent adult neural progenitor cells. Proc. Natl. Acad. Sci. USA 101, 16659–16664.

Hu, W., Qiu, B., Guan, W., Wang, Q., Wang, M., Li, W., Gao, L., Shen, L., Huang, Y., Xie, G., et al. (2015). Direct conversion of normal and Alzheimer's disease human fibroblasts into neuronal cells by small molecules. Cell Stem Cell 17, 204–212.

Ladewig, J., Mertens, J., Kesavan, J., Doerr, J., Poppe, D., Glaue, F., Herms, S., Wernet, P., Kögler, G., Müller, F., et al. (2012). Small molecules enable highly efficient neuronal conversion of human fibroblasts. Nat. Methods 9, 575–578.

Li, X., Zuo, X., Jing, J., Ma, Y., Wang, J., Liu, D., Zhu, J., Du, X., Xiong, L., Du, Y., et al. (2015). Small-molecule-driven direct reprogramming of mouse fibroblasts into functional neurons. Cell Stem Cell *17*, 195–203.

Lindvall, O., and Kokaia, Z. (2006). Stem cells for the treatment of neurological disorders. Nature *441*, 1094–1096.

Liu, M.L., Zang, T., Zou, Y., Chang, J.C., Gibson, J.R., Huber, K.M., and Zhang, C.L. (2013). Small molecules enable neurogenin 2 to efficiently convert human fibroblasts into cholinergic neurons. Nat. Commun. *4*, 2183.

Liu, Y., Miao, Q., Yuan, J., Han, S., Zhang, P., Li, S., Rao, Z., Zhao, W., Ye, Q., Geng, J., et al. (2015). Ascl1 converts dorsal midbrain astrocytes into functional neurons in vivo. J. Neurosci. *35*, 9336–9355.

Mertens, J., Marchetto, M.C., Bardy, C., and Gage, F.H. (2016). Evaluating cell reprogramming, differentiation and conversion technologies in neuroscience. Nat. Rev. Neurosci. *17*, 424–437.

Moretto, G., Xu, R.Y., and Kim, S.U. (1993). CD44 expression in human astrocytes and oligodendrocytes in culture. J. Neuropathol. Exp. Neurol. *52*, 419–423.

Niu, W., Zang, T., Zou, Y., Fang, S., Smith, D.K., Bachoo, R., and Zhang, C. (2013). In vivo reprogramming of astrocytes to neuroblasts in the adult brain. Nat. Cell Biol. *15*, 1164–1175.

Pruszak, J., Sonntag, K., Aung, M.H., Sanchez-Pernaute, R., and Isacson, O. (2007). Markers and methods for cell sorting of human embryonic stem cell-derived neural cell populations. Stem Cells *25*, 2257–2268.

Xu, J., Du, Y., and Deng, H. (2015). Direct lineage reprogramming: strategies, mechanisms, and applications. Cell Stem Cell *16*, 119–134.

Yang, N., Ng, Y.H., Pang, Z.P., Südhof, T.C., and Wernig, M. (2011). Induced neuronal cells: how to make and define a neuron. Cell Stem Cell *9*, 517–525.

Yuan, S.H., Martin, J., Elia, J., Flippin, J., Paramban, R.I., Hefferan, M.P., Vidal, J.G., Mu, Y., Killian, R.L., Israel, M.A., et al. (2011). Cell-surface marker signatures for the isolation of neural stem cells, glia and neurons derived from human pluripotent stem cells. PLoS One *6*, e17540.

Zhang, Y., Pak, C., Han, Y., Ahlenius, H., Zhang, Z., Chanda, S., Marro, S., Patzke, C., Acuna, C., Covy, J., et al. (2013). Rapid single-step induction of functional neurons from human pluripotent stem cells. Neuron *78*, 785–798.

Zhang, L., Yin, J., Yeh, H., Ma, N., Lee, G., Chen, X.A., Wang, Y., Lin, L., Chen, L., Jin, P., et al. (2015). Small molecules efficiently reprogram human astroglial cells into functional neurons. Cell Stem Cell *17*, 735–747.

Zhang, M., Lin, Y., Sun, Y.J., Zhu, S., Zheng, J., Liu, K., Cao, N., Li, K., Huang, Y., and Ding, S. (2016a). Pharmacological reprogramming of fibroblasts into neural stem cells by signaling-directed transcriptional activation. Cell Stem Cell *18*, 653–667.

Zhang, Y., Sloan, S.A., Clarke, L.E., Caneda, C., Plaza, C.A., Blumenthal, P.D., Vogel, H., Steinberg, G.K., Edwards, M.S., Li, G., et al. (2016b). Purification and characterization of progenitor and mature human astrocytes reveals transcriptional and functional differences with mouse. Neuron *89*, 37–53.